Malaysian Journal of Analytical Sciences (MJAS)
Published by Malaysian Analytical Sciences Society

NOVEL ALGINATE-CHITOSAN AMINE-FUNCTIONALIZED SILICA COATED MAGNETIC COMPOSITE FOR HEAVY METALS REMOVAL IN WATER

(Komposit Baharu Alginat Kitosan Difungsikan dengan Amina Bersalut Silika Bermagnet untuk Penyingkiran Logam Berat dalam Air)

Gimba Joshua Dagil[1,2], Ng Nyuk-Ting[1], Aemi Syazwani Abdul Keyon[1,3*]
Wan Aini Wan Ibrahim[1,3*], and Sheela Chandren[1,3]

[1] *Department of Chemistry, Faculty of Science, Universiti Teknologi Malaysia, 81310 UTM Johor Bahru, Johor, Malaysia*
[2] *Department of Science, Plateau State Polytechnic, Barkin Ladi, P.M.B 02023, Bukuru, Jos Nigeria*
[3] *Centre for Sustainable Nanomaterials, Ibnu Sina Institute for Scientific and Industrial Research, Universiti Teknologi Malaysia, 81310 UTM Johor Bahru, Johor, Malaysia*

**Corresponding author e-mail: aemi@utm.my; waini@utm.my*

Received: 15 August 2022; Accepted: 17 January 2023; Published: 19 April 2023

Abstract

A new effective biopolymer alginate chitosan amine-functionalized silica coated magnetic composite (alg/Cs-NH_2-SiO_2/Fe_3O_4) adsorbent was synthesized and applied for the first time to remove Pb(II), Cu(II) and Cd(II) from aqueous solution by utilizing inductive coupled plasma-optical emission spectroscopy (ICP-OES). The properties of the composite were characterized using Fourier-transform infrared spectroscopy (FTIR), Field emission scanning electron microscopy/energy-dispersive X-ray spectroscopy (FESEM/EDX), and vibrating sample magnetometry (VSM). Evaluation of alg/Cs-NH_2-SiO_2/Fe_3O_4 adsorption performance at optimum conditions revealed that the adsorbent had a maximum adsorption capacity of 41.79, 39.21, and 39.56 mg/g for Pb(II), Cu(II) and Cd(II), respectively. The adsorbent behavior was studied using Langmuir, Freundlich, Temkin, and Dubinin-Rudushkevich's isotherm models. The Langmuir isotherm and the pseudo-second-order were better fitted with the coefficient of determination (R^2) value of 0.99, indicating homogeneous surface and chemisorption processes. The thermodynamic factors indicated endothermic and spontaneous processes at 60 °C. Even after the 5th cycle adsorption-desorption experiments, the adsorbent still retained its adsorption ability above 70% metal ions removal, indicating that the adsorbent was reasonable for metal ions removal in water. Pb(II) was detected in a river near an industrial area (Taman Mewah, Kulai, Johor), which was eventually removed by the adsorbent at 86% efficiency.

Keywords: biopolymer, magnetic adsorbent, heavy metals

Abstrak

Penjerap biopolimer alginat kitosan amina bersalut silika bersalut (alg/Cs-NH_2-SiO_2/Fe_3O_4) yang berkesan telah disintesis dan digunakan buat kali pertama untuk menyingkirkan ion Pb(II), Cu(II) danCd(II) daripada air dengan menggunakan spektroskopi pelepasan atomik-plasma gandingan aruhan (ICP-OES). Ciri-ciri komposit dicirikan menggunakan spektroskopi inframerah-

transformasi Fourier (FTIR), mikroskop elektron pengimbasan pancaran medan (FESEM), spektroskopi sinar-X penyebaran tenaga (EDX), dan magnetometri getaran sample (VSM). Penilaian prestasi penjerapan alg/Cs-NH_2-SiO_2/Fe_3O4 pada keadaan optimum menunjukkan bahawa penjerap mempunyai kapasiti penjerapan maksimum 41.79, 39.21, dan 39.56 mg/g masing-masing untuk Pb(II), Cu(II) dan Cd(II). Prestasi penjerap dikaji menggunakan model isoterma Langmuir, Freundlich, Temkin, dan Dubinin-Rudushkevichs. Isoterma Langmuir dan pseudo-tertib kedua adalah lebih bertepatan dengan nilai pekali penentuan (R2) 0.99, menunjukkan permukaan homogen dan proses penjerapan secara kimia. Faktor termodinamik menunjukkan proses endotermik dan spontan pada 60 °C. Walaupun selepas lima kali eksperimen penjerapan-penyahjerapan , penjerap masih mengekalkan keupayaan penjerapannya dengan % penyingkiran ion logam melebihi 70% menunjukkan penjerap berupaya mengeluarkan ion logam daripada air. Pb(II) telah dikesan di sungai berhampiran kawasan perindustrian (Taman Mewah, Kulai, Johor), akhirnya disingkirkan pada kecekapan 86%.

Kata kunci: biopolimer, penjerap magnet, logam berat

Introduction

Clean water resources are undoubtedly a basic human need. However, population growth, industrialization and urbanization, domestic and industrial waste generation, and other anthropogenic sources of toxic pollutants have made many water resources detrimental to humans and the environment. Industries that produce large volumes of effluents include textile, breweries, mineral processing, poultry processors, paper and fiber plants, meat packers, fruit and vegetable packing operations, fertilizer plants, refiningand petrochemical operations, and many more. Wastewaters from these industries generally contain heavy metals,dyes, pesticides and, etc [1]. On top of that, they are soluble in water (i.e. dyes and pesticides), non-biodegradable with a tendency to bioaccumulate (i.e. heavy metals), and are easily transported into the food chain [2]. Having high atomic density >5 g/cm^3, heavy metals could be toxic and poisonous even at trace levels [3]. The rapid increases in contamination by heavy metals from industrial and urban wastewaters are undoubtedly worrying [4, 5, 6].

Techniques such as ion exchange, precipitation, coagulation, and floatation, have been utilized to extract and/or remove various heavy metals from water. However due to the issue of sludge/waste disposal [7], alternative methods arise. The adsorption method has been recognized as one of the promising methods since it only requires a small amount of adsorbent, thus promoting simplicity and efficiency to remove heavy metals from water [8]. It utilizes a mass transfer process through which metal ions are transported from solution onto the surface of a solid material (adsorbent) and become attached via chemical or physical interactions. Various adsorbents have been established and reported based on agricultural wastes, clay, zeolite, activated carbon, biopolymer, and others [9]. A new class of materials; organic-inorganic hybrid materials are attracting interest in creating a high-performing polymeric that shows good possibilities for removal of metal ions through modifications. These modified hybrid materials exhibit better properties than the original components [10]. Additionally, the natural materials of the hybrid, for instance, the agro-wastes products, clay, and biopolymers are environmentally friendly and are widely available to serve as alternative low-cost adsorbents to the commercially activated carbon. The need for a safe and better economical method for heavy metal removal from polluted water has challenged researcher's interest in the production of better low-cost alternatives [11]. Some low-cost agricultural by-products such as sugarcane bagasse and the neem backed, rice husks, sawdust, coconut husks, oil palm shells, etc have been described in the literature for metals removal [12]. To step up the performance of adsorbents from agricultural products, some modifications are needed to enhance their adsorption capacities as adsorbents[13, 14]. This included the utilization of magnetic aspect for nanomaterial adsorbents.

Adsorbents from magnetic nanomaterials (MNPs) usually possess a large surface area, and short diffusion route, without the tediousness of filtration and centrifuging. Easy separation of the adsorbents from water/wastewater using an external magnet makes MNPs reusable. However, the MNPs may suffer agglomeration, oxidation in the air during synthesis, not target-discriminatory towards analytes, and are incompatible

with compounds inside complicated matrices. Hence, they can be enhanced by a suitable coating modification to overcome these limitations [15]. The MNPs can be coated from being oxidized or can be dispersed under low pH conditions by surface coating with silica (SiO_2). SiO_2 is stable under the acid condition and inert to redox reactions as compared to the organic coating substances, and hence serves as an ideal shell composite to safeguard the inner magnetic core. Consequently, the SiO_2 coated layer has numerous hydroxyl groups on its surface which offer the easy possibility of the functionalization of the MNPs without damaging or changing the core of the materials. SiO_2-coating of the core-shell MNPs (Fe_3O_4@SiO_2) has been explored for many applications [15]. Features include stability, reactivity, solubility, melting points, and electronic structure relatively different from their original material to give a homogeneous size and shape as well as regulate its stability in aqueous solutions. APTES has been modified on the surface of silica-coated magnetite to form Fe_3O_4@SiO_2-NH_2 used for Zn(II) removal from contaminated effluent [16]. Mercaptamine had been used in silica coated MNPs to obtain the functionalized composite for Hg and Pb(II) removal [17]. Furthermore, As(III) removal had been achieved using encapsulated magnetite adsorbent in which the covalent bond was modified through the alginate to obtain the carboxylic functionalized adsorbent [18]. To explore the effect of the carboxylic alginate modified method, functionalization of the carboxylic group had also been done to enhance adsorption towards Pb(II) removal [19]. The application of alginate-chitosan-based amine-functionalized silica coated magnetite alg/Cs-NH_2-SiO_2/Fe_3O_4 as adsorbent for the removal of Pb(II), Cu(II), and Cd(II), in aqueous environments is still not explored and is an interesting area in adsorbent synthesis research.

This study was designed to develop a new eco-friendly adsorbent, i.e., the alginate-chitosan-based amine-functionalized silica coated magnetic (alg/Cs-NH_2-SiO_2/Fe_3O_4) adsorbents for the removal of Pb(II), Cu(II) and Cd(II) in water and wastewater. The characterization was conducted on the adsorbent, i.e., FTIR, FESEM/EDX, and VSM to ascertain the synthesis process. The optimization of the adsorption parameters such as sample pH, dosage, initial adsorbate concentration, contact time, and temperature was conducted via the batch adsorptions method. Ultimately, the adsorption, kinetic isotherm, thermodynamic, and reusability studies were done to evaluate the fundamental and economic aspects of the adsorbent. A real sample from an industrial wastewater site was applied to test the ultimate effectiveness of the adsorbent in the real application.

Materials and Methods

Chemicals, reagents, and instrumentations

Iron(III) chloride hexahydrate ($FeCl_3.6H_2O$, 99%), ethanol (99%) iron(II) chloride tetrahydrate ($FeCl_2.4H_2O$, 99%), and sodium hydroxide (NaOH), the stock solution of salts copper, lead, cadmium, alginate (alg), and chitosan (Cs) were bought from Merck (Germany). 3-aminopropyltriethoxysilane (APTES), tetraethyl orthosilicate (TEOS), concentrated NH_4OH (28%), HNO_3(65%), and HCL (37%) were purchased from Fluka Chemical. HCl (0.1M) and/or NaOH (0.1M) were used to adjust the pHs of the solutions. Analytical grade chemicals were used without further purifications. All glassware was soaked in 5% HNO_3 acid for 24 h and rinsed in deionized water to prevent metal contaminations. Several instruments were used and applied for the synthesis of magnetic alg/Cs-NH_2-SiO_2/Fe_3O_4 adsorbents. These include Avio ^{TM} parker 200 Inductive Couple Plasma-Optical Emission Spectrometry (ICP-OES) was used for the metal ions analysis. ATM 400 FTIR spectrometer from PerkinElmer (Waltham, MA, USA) was also utilized for the characterization of the synthesized adsorbents. FTIR estimations utilizing the KBr pellet procedure and transmission mode of all spectra were recorded from 400 to 4000cm^{-1}. A JSM-6701 F electron magnifying instrument from JEOL (Tokyo, Japan) was utilized for the field emission sample electron microscopy (FESEM) analysis, and the energy dispersive X-Ray examination (EDX). Vibrating sample magnetometry (VSM 7400) from Lake Shore Cryotronics (Ohio, USA) was used to evaluate the magnetic properties of the materials at a utilized greatest field of 15,000 G at room temperature.

Synthesis procedures

The synthesis of iron oxide (Fe_3O_4NPs) was by simple

co-precipitation procedure [20, 21]. This was done by mixing 8.48 g of $FeCl_3.6H_2O$ and 2.25g of $FeCl_2.4H_2O$ in a three-necked round bottom flask and stirring vigorously under argon gas at a temperature of 80 ℃ in a 100 ml volume of deionized water. Subsequently, 24 ml of ammonia (25%) was dropwise added under a constant mechanical stirring for 5 h to form black magnetic oxide (Fe_3O_4) at room temperature. The as-prepared Fe_3O_4 was washed with distilled water and methanol, separated with an external magnet, and finally oven-dried at 60 ℃ for 24 h. The final product was then kept for further experiments in an airtight container. The preparation of SiO_2/Fe_3O_4NPs was done by re-dispersing [22] 1.0 g of the Fe_3O_4NPs in deionized water (50 ml) under argon for 10 mins. After a continuous stirring of the products, TEOS (1 ml) diluted in ammonium hydroxide (2 ml) was finally added dropwise to the dispersion with more continuous mechanical stirring at room temperature for 14 h. The magnetic Fe_3O_4/SiO_2 mixture was then washed with ethanol and water and finally collected by external magnetic separation, then dried overnight in a furnace at 110 ℃.

The Cs-Fe_3O_4NPs was prepared by dissolving 2.0 g chitosan in 100 ml (2%) concentration of acetic acid to form a homogeneous solution. The content was then transferred to a three-necked flask under vigorous mechanically stirring followed by adding 20 ml of glutaraldehyde (5% wt solution) for 4 h. The Cs-Fe_3O_4 NPs formed were recovered by an external magnetic separation. The particles were allowed to settle for at least 2 min before being washed with water/ethanol about three times before finally dried in a vacuum oven at 50 ℃. The preparation of Cs-NH_2-SiO_2/Fe_3O_4 was made by dispersing 2.0 g of Cs-Fe_3O_4 in deionized water (100 ml) followed by 20 ml of APTES with vigorous mechanical stirring of the mixture at 40 ℃ for 1 h. The mixture was left overnight with vigorous stirring followed by vacuum filtration the next day and finally, oven-dried at 50 ℃ and stored for future use. Then, the preparation of the final alg/Cs-NH_2-SiO_2/Fe_3O_4 was done by dispersing 2.0 g of Cs-NH_2-SiO_2/Fe_3O_4 in deionized water (100 ml) under vigorous mechanical stirring of the mixture at 40 ℃ for 1 h. A solution containing 50 ml 0.1M $CaCl_2$ was then added dropwise by using a needle syringe to the resultant mixture in a beaker for the formation of the beads. The beads were then soaked 0.1 M $CaCl_2$ solution overnight and then washed thoroughly with distilled water, oven-dried overnight at a temperature of 50 ℃, and finally stored for further use. The proposed schematic synthesis route is presented in Figure 1.

Batch sorption experiments for metal ions adsorption

Adsorption experiments of Pb(II), Cd(II), and Cu(II) onto the newly synthesized alg/Cs-NH_2-SiO_2/Fe_3O_4 were carried out using the batch sorption method. The influence of solution pH, adsorbent dosage, contact time, temperature, and initial concentration of adsorbate was studied. 100 mL conical flasks holding 50 mL solutions of different metal ions with initial concentrations varying from 20 -100 mg/L, and fixed adsorbent dosage of 20 mg was used for the equilibrium experiments. The solution pH was set at pH 6, then shaked at an equilibrium contact time of 30 min, and temperature at 25 ℃, to establish equilibrium after which, an external magnet was used to separate the adsorbents from their respective solutions. The solutions were analyzed using an ICP-OES instrument for the residual heavy metal ions concentrations, and all experiments were conducted in triplicate. The percentage removal (%R) and the adsorption capacity (q_e) according to equations 1 and 2, respectively [24].

$$\%R = \frac{[(C_i - C_f)]}{C_i} x\ 100 \quad (1)$$

$$q_e = \frac{[(C_i - C_f)]\,V}{m} \quad (2)$$

Where, V = volume of solution (mL), qe = the adsorption capacity in (mg/g), m= quantity of adsorbent (mg), Ci = initial concentration of metal ions (mg/L), and Cf = final concentration of metal ions (mg/L).

Regeneration studies and wastewater samples treatment

The adsorption-desorption experiment for five consecutive rounds of regeneration study was conducted

until a substantial change in the performance of alg/Cs-NH_2-SiO_2/Fe_3O_4 was detected. Consequently, the adsorbed metal ions were desorbed in 5 mL HCL (0.1M), after each 5 min shaking to retrieve the adsorbent from the mixture with an external magnet, then washed with deionized water until neutral, and finally, oven-dried at 60 ºC for 24 h. ICP-OES instrument was used to investigate the residual concentration of heavy metal pollutants in the mixtures [25]. The efficiency of the alg/Cs-NH_2SiO_2/Fe_3O_4 adsorbent towards Pb(II), Cd(II), and Cu(II) from real wastewater effluents was investigated using effluents from industrial locations along the Skudai river at Taman Mewah, Kulai, Johor, Malaysia. The floating solids were eliminated through filtration. HNO_3 was utilized to digest the test samples to further eliminate matrix interferences. The metal ions residual concentrations in the samples were determined after the adsorption experiment using the synthesized adsorbent.

Results and Discussion

Synthesis route for alg/Cs-NH_2-SiO_2/Fe_3O_4 adsorbent

The alg/Cs-NH_2-SiO_2/Fe_3O_4 adsorbent was synthesized from Fe_3O_4, as a percussor coated with SiO_2, functionalized using APTES (-NH_2), blend combined with Cs, and the bound by alg to form a biopolymer composite adsorbent. The schematic synthesis route of alg/Cs-NH_2-SiO_2/Fe_3O_4 was through five steps namely, Fe_3O_4 was successfully synthesized by mixing $FeCl_3.6H_2O$ and $FeCl_2.4H_2O$). SiO_2/Fe_3O_4 was prepared from Fe_3O_4 and TEOS in diluted ammonium hydroxide. NH_2-SiO_2/Fe_3O_4 was prepared through SiO_2/Fe_3O_4 and APTES. Cs-NH_2-SiO_2/Fe_3O_4 was prepared chitosan in 100 ml (2%) concentration of acetic acid via cross-linking by glutaraldehyde. Finally, the adsorbent alg/Cs-NH_2-SiO_2/Fe_3O_4 was successfully prepared through Cs-NH_2-SiO_2/Fe_3O_4 by forming a composite with the addition of alginate. (Figure 1).

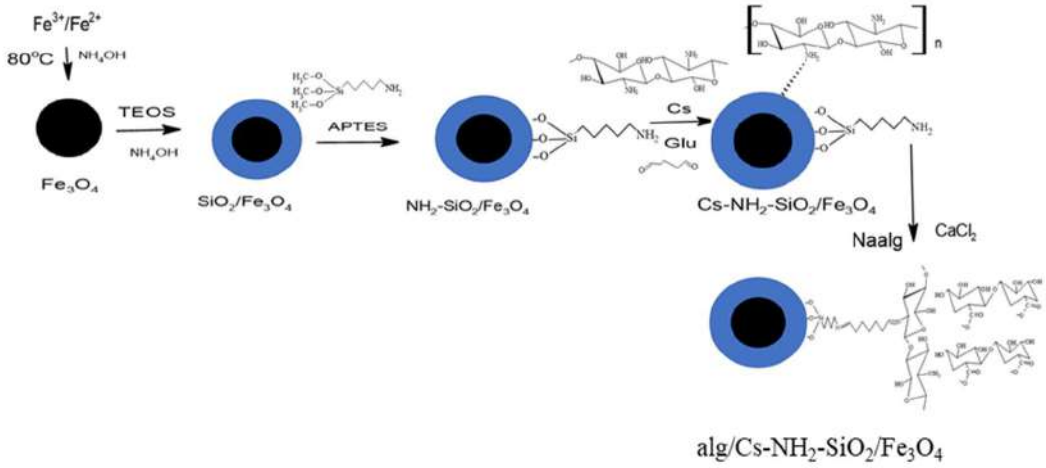

Figure 1. Schematic synthesis route of alg/Cs-NH_2-SiO_2/Fe_3O_4 adsorbent

Characterization of the synthesized alg/Cs-NH_2-SiO_2/Fe_3O_4 adsorbent

To determine the functional groups in the newly synthesized adsorbent, FTIR analysis was conducted. The FTIR spectra of the raw Cs and alg were compared to the newly synthesized material as indicated in Figure 2(a-b). The peaks for raw Cs at 3451 cm^{-1}, 2925-2885 cm^{-1}, 1652 cm^{-1}, and 1371 cm^{-1} were ascribed to the overlapping between -NH_2 and -OH stretching vibration and the intermolecular hydrogen bonding of the polysaccharide, C-H stretching vibrations of C=O saturated carbons, in acetamide group, and C-O group stretching and C-H bending vibrations. The main spectrum of raw alg (Figure 2(b)) shows 1624 cm^{-1}, 1421 cm^{-1}, and 1014 cm^{-1} which corresponds to C-H vibrational stretch and C=O vibrational stretch. The spectrum of Fe_3O_4 (Figure 2(c)) showed a peak at 574 cm^{-1} for Fe-O bond formation. The spectrum of SiO_2/Fe_3O_4 (Figure 2(d)) showed O-H

vibration, C-H stretching, C-H bending, C-O stretching peaks, Fe-O bond at 3429 cm^{-1}, 1624 cm^{-1}, 1400 cm^{-1}, 1300 cm^{-1}, and 574 cm^{-1}. Additionally, alg/Cs-NH_2-SiO_2/Fe_3O_4 showed the spectra changed with O-H vibration, C-H stretching, C-H bending, C-O stretching peaks, and Fe-O bond formation at 3149 cm^{-1}, 1542 cm^{-1}, 1053 cm^{-1}, and 596 cm^{-1}, respectively. Key findings showed that the spectra at 1658 cm^{-1}, 1025 cm^{-1}, and 623 cm^{-1} disappeared and the formation of new peaks of 1542 cm^{-1}, 1404 cm^{-1}, 1053 cm^{-1}, and 596 cm^{-1}, respectively corresponded to -NH_2,-C=O, Si-O-Si, and Fe-O, respectively, (Figure 2(f-g)), confirming new material. Consequently, the FTIR spectra of alg/Cs-NH_2-SiO_2/Fe_3O_4 presented peaks at 3400 cm^{-1} and 3200 cm^{-1} for O-H stretching and H_2O molecules, respectively, conformed to the findings of others reported in the literature [26].

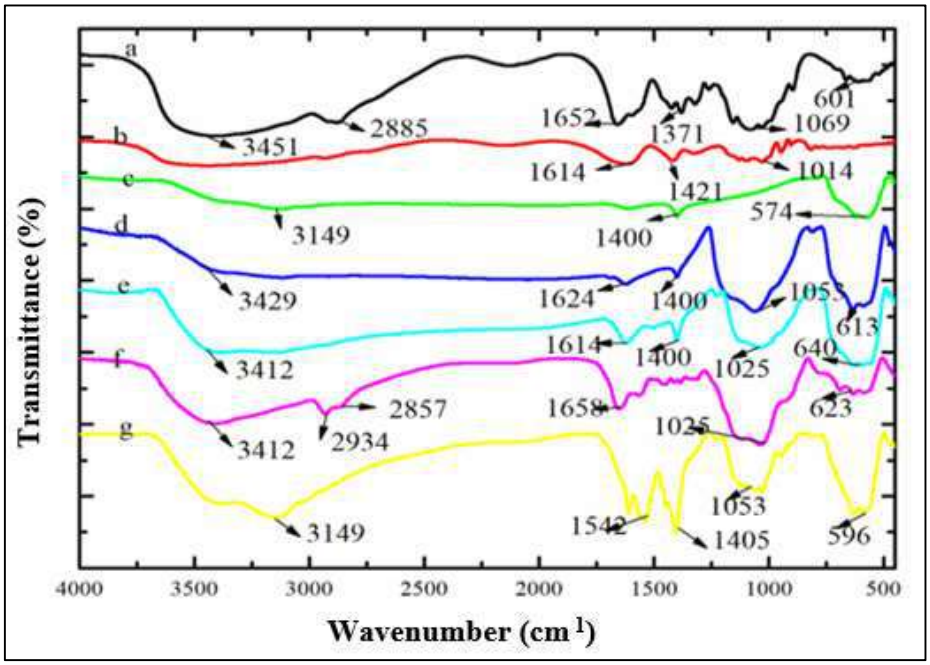

Figure 2. FTIR spectra of (a) chitosan (Cs), (b) alginate (alg) (c) Fe_3O_4, (d) SiO_2/Fe_3O_4, (e) NH_2-SiO_2/Fe_3O_4 (f) Cs-NH_2-SiO_2/Fe_3O_4 (g) alg/Cs-NH_2-SiO_2/Fe_3O_4 adsorbent

The FESEM/EDX analysis was conducted to investigate the surface morphology, particle size distributions, and the relative shape of the synthesized materials. The morphologies and the spectra of Fe_3O_4, SiO_2/Fe_3O_4, NH_2-SiO_2/Fe_3O_4, Cs-NH_2-SiO_2/Fe_3O_4, and alg/Cs-NH_2-SiO_2/Fe_3O_4 are shown in Figure 3(a-j). FESEM morphology of Fe_3O_4 (Figure 3a) showed spherical particle distribution with an average grain size range of 11-14 nm nanosized particles. The EDX spectra of Fe_3O_4 (Figure 3(b)) confirmed the element of Fe (69.20%), and O (17.70%). The FESEM morphology of SiO_2/Fe_3O_4 (Figure 3(c)) was much smoother with an increase in the nanosized average diameter of 15 - 16 nm due to the silica coatings on the surface of the magnetite, while the EDX spectra of SiO_2/Fe_3O_4 (Figure 3(d)) confirmed the element of Fe (55.50%), O (34.50%), and Si (3.5%) confirming the coating of SiO_2 on top of the magnetite during the synthesis process. The similar obs ervations were also reported by other researchers [27]. With the addition of APTES to the SiO_2 coated magnetite, the size distribution increased with changes in shape to particle diameter size range of 18-23 nm due to the -NH_2 functionalization of SiO_2/Fe_3O_4. This was well confirmed by the FTIR spectra and the EDX of NH_2-$SiO_2Fe_3O_4$ (Figure 3(f)) containing Fe (38.4%), O (43.4%), Si (4.2%), and N (1.5%) which showed the

functionalization of the SiO_2/Fe_3O_4 with APTES due to the presence of the N element. Furthermore, with the addition of Cs and alg to form alg/Cs-NH_2-SiO_2/Fe_3O_4, the FESEM morphology (Figure 3(i)) showed a more distinctive particle size distribution and shape with a denser and larger particle diameter size range of 23-50 nm and 121-148 nm, respectively. The addition of Cs and alg introduced the element of C (56.2%) (Figure 3(h) and Figure 3(j) owing to the existence of the functional groups of -NH_2 and -OH, respectively. FESEM morphology of alg/Cs-NH_2-SiO_2/Fe_3O_4 (Figure 3(i)) showed the gel formation due to the glutaraldehyde cross-linking resulting in a darker morphology with the largest diameter distribution of 114-148 nm with an oval shape liked morphology quite different from the others in conformity with other reported findings [27]. Undoubtedly, the % elemental composition of Fe, O, and Si continued to decrease with an increase in the diameter of the core-shell of the adsorbent; nevertheless, the magnetism of the final adsorbent was reasonable for removal work (Figure 4).

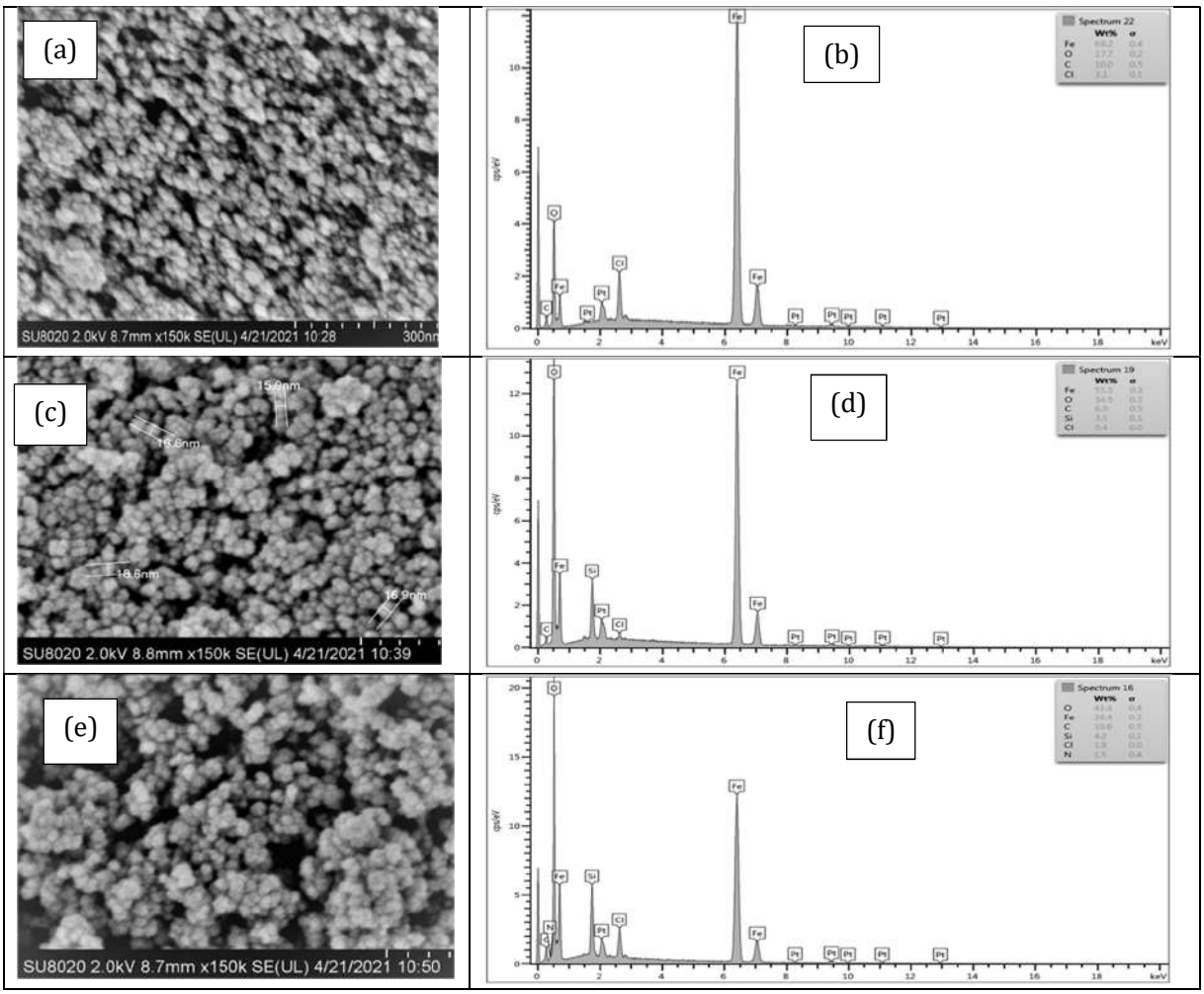

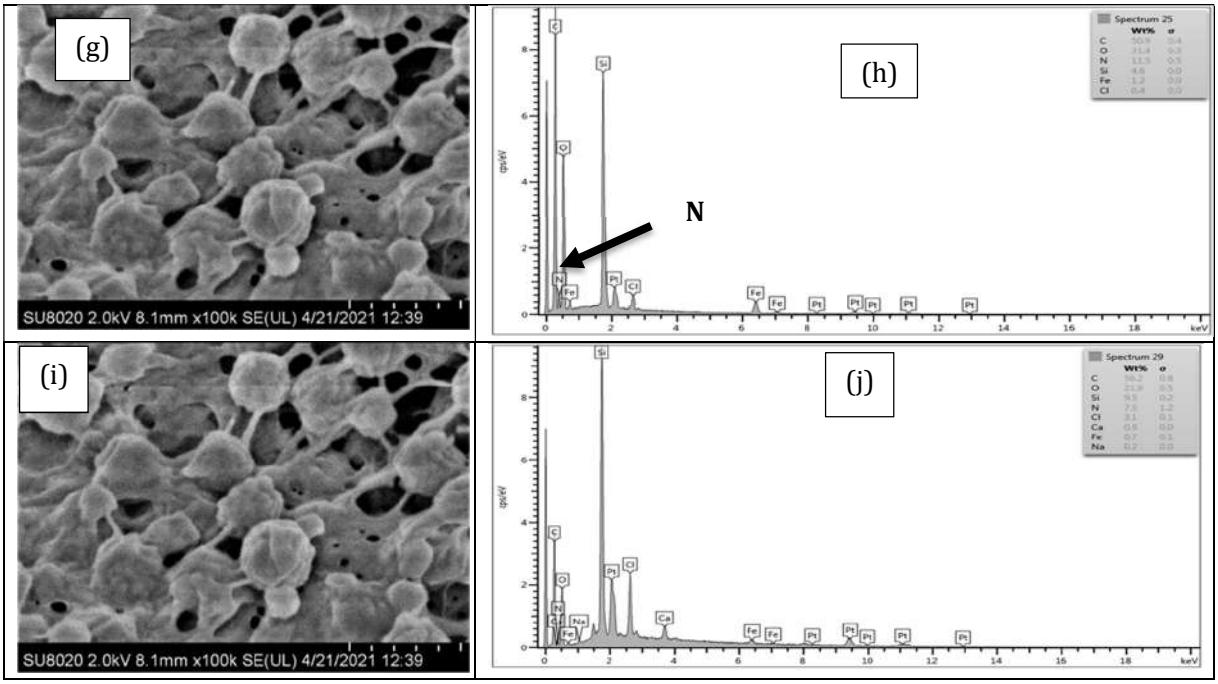

Figure 3. FESEM morphology and EDX spectra of (a-b) Fe_3O_4, (c-d) SiO_2/Fe_3O_4, (e-f)NH_2-SiO_2/Fe_3O_4, (g-h) Cs-NH_2-SiO_2/Fe_3O_4 and (i-j) alg/Cs-NH_2-SiO_2/Fe_3O_4 adsorbents Magnification. = 100K or 150K

The magnetization curves of Fe_3O_4, N H_2-SiO_2/Fe_3O_4, and alg/Cs-NH_2-SiO_2/Fe_3O_4 adsorbents were investigated via VSM polarization for before and after adsorption in the range of −15000 to 15000KOe. The magnetic hysteresis loops of Fe_3O_4, NH_2-SiO_2/Fe_3O_4, and alg/Cs-NH_2-SiO_2/Fe_3O_4 demonstrated the superparamagnetic characteristic of the materials with saturation magnetization values of 24.48, 20.10 and 14.77 emu/g, respectively (Figure 4(a-c)). The results revealed that the adsorbent alg/Cs-NH_2-SiO_2/Fe_3O_4 displayed sufficient magnetic quality to achieve magnetic separation. Hence, the VSM bends S-shape showed super-paramagnetic properties for nanocomposite well suitable for the assortment of magnetic adsorbents from aqueous solution. The decrease in the saturation magnetization values from Fe_3O_4 to alg/Cs-NH_2-SiO_2/Fe_3O_4 was due to the various modification that had taken place on top of the Fe_3O_4. Although the saturation magnetization value decreased after the immobilization process, the adsorbent responded rapidly to an external magnet and could be separated from the aqueous mixture conveniently within 45 seconds in agreement with the similar finding reported by [28].

Optimization of adsorption using the newly synthesized alg/Cs-NH_2-$SiO_2Fe_3O_4$ adsorbent

The impact of variables such as the sample pH, dosage, initial adsorbate (metals ion) concentration, contact time, and the temperature for the adsorption of selected metal ions using alg/Cs-NH_2-SiO_2/Fe_3O_4 adsorbent was analyzed and optimized utilizing the batch adsorption technique (Figure 5a-e).

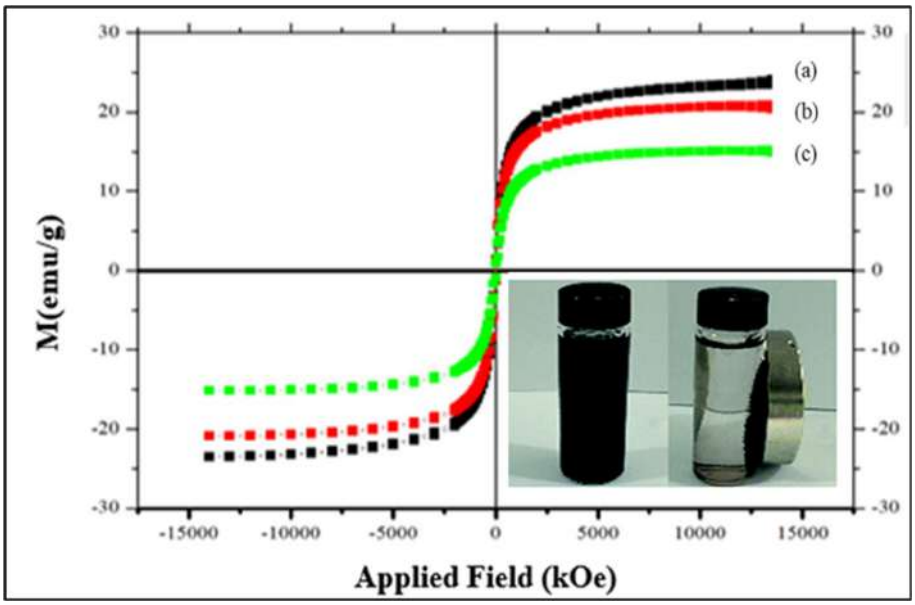

Figure 4. VSM plot for (a) Fe_3O_4 (24.48 emu/g), (b) NH_2-SiO_2/Fe_3O_4 (20.10 emu/g), (c) alg/Cs-NH_2-SiO_2/Fe_3O_4 (14.77 emu/g). The photo showed the separation of adsorbent using an external magnet.

A key to optimizing parameters in the process of metal ions adsorption onto the adsorbent was the pH of the water solution. The effect of pH was conducted by varying the pH from 2-7 and keeping other factors constant (Figure 5a). The findings revealed a maximum pH of 6 with % of metal ions removal for Pb(II), and Cd(II), except pH 7 for Cu(II) with the value of 73.74%, 68.82%, and 66.68% respectively. The adsorbent oxygenated active sites of Cs and alg were $–NH_2$, -OH, and –COOH. At lower pH, protonation occurred at the active sites of the adsorbent, and there was a competition between the protonated (H^+) active sites of the adsorbent and M^{2+} ions which induced electrostatic repulsion between the protonated sites (H^+) and M^{2+}, in turn, reduced quantity of adsorption of the metal. At greater pH values, there were the precipitations of the M^{2+} to form $M(OH)_2$, which resulted in less % metal ions adsorption with a similar pattern to other researchers [29]. Consequently, the value for optimum pH was found to be pH 6. Therefore, pH 6 was most acceptable and used in the next optimization parameter. The influence of contact time on the Pb(II), Cd(II), and Cu(II) adsorption onto alg/Cs-NH_2-SiO_2/Fe_3O_4 adsorbent was investigated. Contact time varied from 20-80 mins (Figure 5b).Time was varied while keeping other conditions constant to maximize the efficiency of the removal due to the time factor. The optimum contact time was achieved at 30 mins with % metal ions removal for Pb(II), Cd(II), and Cu(II) of 78.68, 70.66, and 70.88%, respectively. The fast % metal ions removal at the initial increased due to an abundance in the active accessible sites on the adsorbent surface for interaction with the metal ions. The adsorption accessible to active sites gradually reduced, and the interaction forces were weakened, resulting in a decrease in removal %. This observation was similar to the trends reported by some researchers that metal ions removal increased within the first few minutes of contact with the adsorbent surface [30]. Consequently, 30 mins was selected for the next optimization experiment.

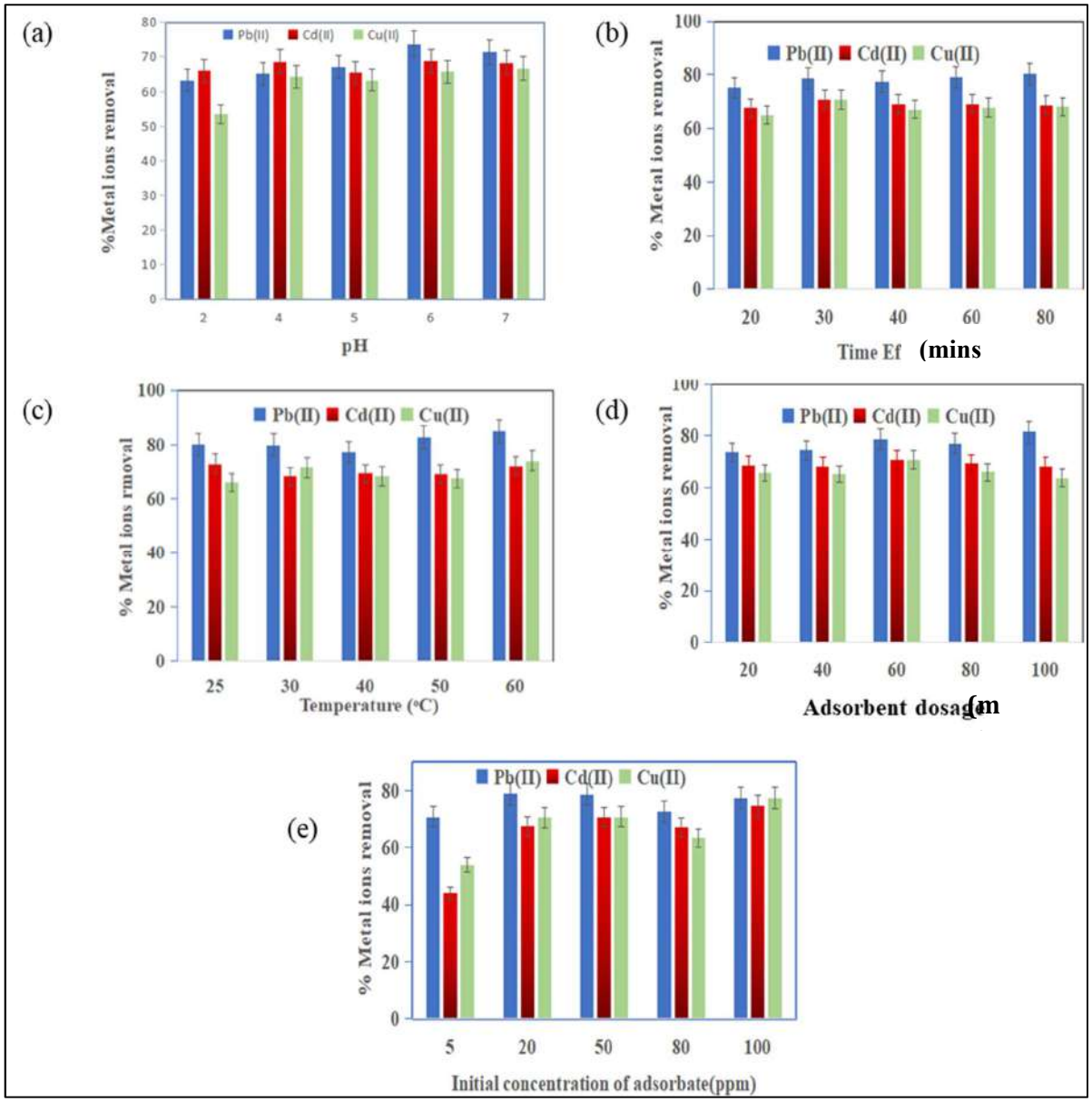

Figure 5. Effect of adsorption parameters (a) pH, (b) time effect , (c) temperature, (d) adsorbent dosage, and (e) initial concentration of adsorbate using alg/Cs-NH_2-SiO_2/Fe_3O_4 adsorbent for Pb(II), Cd(II) and Cu(II) removal in water.

The temperature effect on the removal process was a critical optimization parameter because the forces of interactions between adsorbate and adsorbent are either weakened or strengthened with changes in temperature or heat. Additionally, the mobility of metal ions increases with temperature and the affinity of the metal ions at a higher temperature also increased for most magnetic nanocomposites. A series of tests were conducted to study the effect of temperature from 20 - 60 ℃ to find the suitable temperature with the best efficiency of the removal (Figure 5c). The results showed that the optimum was achieved at 60 ℃ with % of the metal ions

of 84.76, 72.10, and 73.96 % for Pb(II), Cd(II), and Cu(II), respectively. The increasing temperature with an increase in the metal ions removal % was attributed to endothermic reactions, [31] as well as the increase in the rate of diffusion of the metal ions at greater temperatures[32]. The temperature at 60 °C was selected for the next parameter optimization. To evaluate the influence of the adsorbent dose on the removal process, the adsorbent amount varied from 20 -100 mg (Figure 5d). It was found that the optimum dosage was achieved at 60 mg, with metal ions removal % of 70.66, 78.68, and 70.88% Pb(II), Cd(II), and Cu(II), respectively. The amount of adsorbent dose was found to increase with the increase in available active sites and vice versa [33]. Consequently, 60 mg was the most appropriate dosage and was therefore adopted as the optimum dosage value for the next experiment. The effect of the initial adsorbate concentration was a crucial optimization parameter to increase the adsorbate active sides for the removal process. Concentrations from 5-100 ppm were investigated (Figure 5e). The results showed that the adsorption equilibrium was reached when the initial adsorbate concentration used was 50 ppm; the heavy metals ion % was 78.68, 70.66, and 70.88 % for Pb (II), Cd(II), and Cu(II), respectively. This agrees with the reports of others that the adsorption of metal ions increased with increasing concentrations due to the increasing availability of metal ions competing for the adsorbents active sites i.e. the more the adsorbate concentration the more the amount of the metal ions to be removed by the active sites of the adsorbent and vice versa[34]. Hence, 50 ppm was selected to be used in the next optimization temperature parameter.

Isotherm study

The equilibrium adsorption experiments of Pb(II), Cd(II), and Cu(II) onto the synthesized adsorbents alg/Cs-NH_2-SiO_2/Fe_3O_4 were studied using Freundlich, Langmuir, Temkin, and Dubinin-Radushkevich (D-R-K) isotherms models as a time function of initial concentrations at optimum conditions. Freundlich isotherm presumes multilayer and heterogeneous adsorption sites and it assumed physisorption observed adsorption mechanism [35, 36,37]. The Freundlich straight plot of the equation is given by the equation 3.

$$logq_e = logk_F + \frac{1}{n} logC_e \quad (3)$$

Where q_e and Ce are the quantity of adsorbate adsorbed per mass of the adsorbent (mg/g), and the equilibrium adsorption capacity of the metal ions pollutants (mg/L), respectively, K_F and n are the Freundlich constant suggestive of adsorbent adsorption capability (mg/g), and the heterogeneity factor, correspondingly. The isotherm findings provided the proper understanding of the kind and mechanism of the interaction behavior between the adsorbent and the adsorbate thus, additional explained the mechanism. That is the affinity of adsorbent, surface properties, and the types of the most appropriate adsorption process. The straight plots of *log* q_e against *log* C_e for Pb(II), Cd(II), and Cu(II), respectively, K_F and n for the separate metal ions were computed from intercept *(log* q_e*)* and slope *(1/n)* of the straight away lines (Table 1). The coefficient of regression (R^2) quantities were not close to unity and the KF quantities were not in harmony with the q_e experimental values. Accordingly, the Freundlich model could not sufficiently describe the adsorption processes. The extent of non-linearity between the solution concentration and adsorption was indicated by n values as shown; if $n=1$ indicated the adsorption is linear, if $n < 1$, indicated the adsorption process is through chemisorption, and if $n>1$, was for physical adsorption. Thus, $0 < n > 1$ is hereby appropriate[37]. Langmuir isotherm was established on the assumptions of monolayer and even distribution of adsorption sites on the adsorbent. Consequently, a saturation value may be achieved beyond which no extra adsorption will occur. Additionally, it was assumed that adsorption occurs through chemisorption at any given homogeneous site without interactions between the adsorbed molecules [37]. The linear Langmuir form is given by equation 4.

$$\frac{C_e}{q_e} = \frac{C_e}{q_m} + \frac{1}{q_m k_L} \quad (4)$$

Where q_m and q_e are the optimum adsorption capacity (mg/g), and the experimental adsorption capacity (mg/g), respectively, kL is the linear Langmuir constant (L/mg) and Ce is the concentration (mg/L) of residual solution. The linear plot of Ce/q_e against C_e gives a straight plot

line with an R^2 value for all the metal ions for Pb(II), Cd(II), and Cu(II) in that order. Here, values of qm and kL are computed from the linear slope ($1/qm$) and the intercept ($1/qmkL$). The findings of the adsorption procedures which fitted the Langmuir model based on the established R^2 values were close to 0.999 for Pb(II), Cd(II), except for Cu(II) < 0.999 as demonstrated in Table 2. Additionally, the experimental qe values for Pb(II) and Cd(II) were 41.8 and 39.2 mg/g, respectively, and they agreed with the calculated qm values of 39.4 and 36.6 mg/g, in that order, validating the Langmuir model's suitability to describe the adsorption processes [37,38]. The exception was Cu(II), where the experimental and calculated qe values were 39.6 and 15.6 mg/g. A separation factor constant (R_L) was introduced furthermore, to evaluate the degree of suitability of the adsorbent towards adsorbate and is described by equation 5.

$$R_L = \frac{1}{1+K_L C_o} \quad (5)$$

where K_L(L/mg) and C_o(mg/L) represent the Langmuir constant and the initial adsorbate concentration, respectively. The magnitude of R_L represents the feasibility of adsorption (Table 2). The dimension of R_L was additionally used, for the adsorption studies, if $R_L > 1$, the value indicated the adsorption is unfavorable, $R_L = 1$, indicated the adsorption is linear, and $R_L < 1$, indicated adsorption is favorable. Consequently, where $0 < R_L < 1$ confirmed R_L to be good and applicable for this study [37]. Additionally, the Temkin and the D-R-K isotherms data could not adequately explain the adsorption process of Pb(II), Cd(II), and Cu(II) onto the synthesized adsorbents alg/Cs-NH_2-SiO_2/Fe_3O_4 because of both R^2 < 0.99 (Table 1).

Table 1. Adsorption isotherm model parameters for Pb(II), Cd(II), and Cu(II) adsorption onto alg/Cs-NH_2-SiO_2/Fe_3O_4

Model	Isotherm Constant	Pb(II)	Cd(II)	Cu(II)
Freundlich	n	0.655	0.749	0.741
	k_F (mg/g)	32.0	36.5	32.0
	R^2	0.837	0.801	0.848
Langmuir	q_e (mg/g)	41.8	39.2	39.6
	R_L (mg $^{-1}$)	7.201	8.149	0.937
	R^2	0.998	0.999	0.693
	Calc qm (mg/g)	39.4	36.6	15.6
	R_L (x10^{-3})	2.760	2.440	20.640
Temkin	A	7.123	14.658	10.440
	b	169.455	203.313	202.659
	R^2	0.877	0.801	0.867
D-R-K	q_D (mg/g)	41.79	39.21	39.56
	β (mol^2/J^2)	1.21x10^7	2.58x10^7	8.36x10^6
	R^2	0.36	0.48	0.76

Kinetics study

The adsorption kinetics provides crucial information about the effective design of the time-dependent batch adsorption system [38]. To examine the adsorption kinetics of the synthesized adsorbent, the pseudo-first-order and pseudo-second-order were studied. By using a predetermined concentration of 50.0 mg/L for each of the metal ions concentrations range and a predetermined adsorbent (60.0 mg) dose, the kinetics experiments were done.

The kinetics of adsorption for Pb(II), Cd(II), and Cu(II) onto alg/Cs-NH_2-SiO_2/Fe_3O_4 was examined using Pseudo-first-order linear equation 6.

$$log(q_e - q_t) = log(q_e) - \frac{tK_1}{2.303} \quad (6)$$

Where q_e and q_t are the capacity of adsorption and the quantity of metal ions removal at equilibrium (mg/g), and the quantity of metal ions removal (mg/g) at time t (min), respectively. K_1 is the pseudo-first-order rate constant (min^{-1}) [38]. The straight plots line of *log(qe-qt)* against *t* of pseudo-first-order rate equation for Pb (II), Cd (II), and Cu (II), respectively, along with the quantities of R^2 and k_1 for the corresponding metal ions, q_e and k_1 were calculated from the slope ($-k_1/2.303$) and $ln(q_e)$ as intercepts was summarized (Table 3). Consequently, the R^2 values were < 0.999 implying that the model could not be used to adequately explained through the adsorption process.

The straight-away kinetics equation for pseudo-second-order of Pb(II), Cd(II), and Cu(II), uptake onto alg/Cs-NH_2-SiO_2/Fe_3O_4 was depicted in equation 7.

$$\frac{t}{qt} = \frac{1}{k_2 q_e^2} + \left(\frac{1}{qe}\right) t \quad (7)$$

The straight-line plot relationship of *t/qt* versus *t* straight plot for pseudo-second-order rate equation for Pb(II), Cd(II), and Cu(II), separately. Where q_e and q_t are the adsorption capacity of metal ions adsorbed at equilibrium (mg/g), and the adsorption capacity of metal ions removal (mg/g) at time *t* (min), respectively. Furthermore, k_2 is pseudo-second-order rate constant (g/mg min)[38]. The R^2 estimations for the metal ions were closer to unity, suggesting theappropriateness of the model to explain the adsorption process. Where k_2 and q_e are computed from intercept ($1/k_2 q_e^2$) and slope ($1/q_e$) correspondingly, (Table 2). Consequently, the breakthroughs discovery confirmed that the removal process was the chemisorption-regulated process in agreement with other works reported [38].

Table 2. Kinetic data parameters for Pb(II), Cd(II), and Cu(II) adsorption onto alg/Cs-NH_2-SiO_2/Fe_3O_4

Model	Parameter	Pb(II)	Cd(II)	Cu(II)
Pseudo-first- order	q_e (mg/g)	40.8	35.6	35.8
	k_L (min^{-1})	0.004	0.314	0.402
	R^2	0.39	0.24	0.59
Pseudo-second order	q_e (mg/g)	38.6	36.4	33.6
	k_2 (min^{-1})	-0.95	0.03	-0.06
	R^2	0.99	0.99	0.99

Thermodynamic study

The thermodynamic factors describe the role of temperature control on the Pb(II), Cd(II), and Cu(II) adsorption process towards the produced alg/Cs-NH_2SiO_2/Fe_3O_4, thus, establishing the practicability and workable energy requirement for the adsorption process. The thermodynamics explained the effect of the factors such as the entropy changes (ΔS), enthalpy changes (ΔH), and Gibbs free energy (ΔG), which endorse the type of the adsorption, either one of randomness or non-randomness, endothermic, or exothermic, as well as spontaneous or non-spontaneous. These factors were established using Van't Hoff equation and Gibbs free energy [39], by an operating temperature range of 313-333K at optimum conditions according to equations 8, 9, and 10.

$$lnK_C = \frac{\Delta H}{RT} + \frac{\Delta S}{R} \quad (8)$$

$$\Delta G = -RTlnK_C \quad (9)$$

$$K_C = \frac{q_e}{C_e} \quad (10)$$

Where q_e and C_e are adsorption capability in mg/g and residual analyte (mg/L) concentration after adsorption, respectively. *T* represents the temperature *(K),* and *R* stands for the general gas constant (8.3145J/mol.K = 8.314x10^{-3} kJ/mol.K), K_C is the equilibrium constant. To assess the thermodynamic parameters of the target adsorbates on the as-synthesized adsorbent, the

adsorption isotherms at various temperatures (313, 323, 333K) were conducted. The straight plot of lnK_C versus *1/T* gives a straightaway line plot with an R^2, as represented. The negative quantity of slope suggested the adsorption method is endothermic type. The quantities of ΔH, as well as ΔS, were achieved from the slope ($\Delta H/R$ = - *slope*) and intercept ($\Delta S/R$ = intercept) of the straight linear plot, correspondingly [40]. The values of ΔG (kJ/mol), ΔH (kJ/ mol), and ΔS (J/mol.k), for removal of the heavy metal's ion onto alg/Cs-NH_2-$SiO_2Fe_3O_4$ (Table 3). The positive value of ΔH for the adsorption process of metal ions suggests the endothermic nature of the adsorption process with the order Pb(II) > Cd(II) > Cu(II) at 313K. This also supported the adsorption process with temperature increasement. The positive quantities of ΔH confirmed that the interaction was endothermic and the positive quantities of ΔS provide randomness attraction [40]. The positive value of ΔS was observed for the adsorption process of the metal ions indicating an increase in randomness at the solid/solution interface during the adsorption process with the order Cd(II) > Pb(II) > Cu(II) at 313K. Negative amounts of ΔS demonstrate s the rise in the randomness of the solid/solution boundary through the adsorption process, while the negative amounts of ΔG endorse that the adsorption process is spontaneous. The negative value of ΔG indicated the spontaneity of the adsorption process with the order Pb(II) > Cd(II) > Cu(II) at 313K. Generally, the change in standard free energy is in the range of -20 to 0KJ/mol and for chemisorption varies between -80 to -400Kj/mol. The results corrosions to spontaneous physical adsorption of the metal ions which indicated the system does not gain energy. In addition, ΔH of 4.0 - 8.0 kJ/mol and 8.0 - 40.0 kJ/mol are related to Van der Waals connections and hydrogen bonding, respectively. Accordingly, ΔH for chemisorption started at 40.0 kJ/mol[35]. Consequently, adsorption is a chemisorption-regulated process (Table 3).

Table 3. Thermodynamic factors for Pb (II), Cd (II), and Cu (II) adsorption onto alg/Cs-NH_2-SiO_2/Fe_3O_4 with temperature variations

Analyte	$T(K)$	R^2	ΔG (kJ/mol)	ΔH (kJ/mol)	ΔS (kJ/mol.K)
Pb (II)	313	0.987	-1.855	+2.032	+3.990x10^3
	323		-1.883		
	333		-2.414		
Cd (II)	313	0.975	-1.787	+1.411	+8.171x10^3
	323		-1.519		
	333		-1.403		
Cu (II)	313	0.894	-0.436	+0.868	-7.569x10^3
	323		-0.594		
	333		-1.081		

Regeneration and real samples analyses

The regeneration of an adsorbent was a crucial parameter that makes it more cost-effective in the practical application to remove metal ions from water with a good recovery. In this study, the newly synthesized adsorbent was evaluated for five consecutive cycles using 5.0 ml (0.1M) HCL**.** The results of the Pb(II), Cd(II), and Cu(II)% removal by alg/Cs-NH_2-SiO_2/Fe_3O_4, adsorbent could efficiently be reused for up to 5 cycles, retaining about 70% of its potential. Consequently, the adsorbent was deemed favorable material for use in metal removal from real wastewater. Pb(II) was detected in a holding pond near an industrial area (Taman Mewah, Kulai, Johor), eventually removed by the adsorbent at 86% where by, Cd(II) and Cu(II) were not detected. The adsorbent (alg/Cs-NH_2-

SiO_2/Fe_3O_4) adsorption capacity towards Pb(II), Cd (II), and Cu(II) was compared with other adsorbents in the literature (Table 4). This adsorbent compared fairly with its contemporaries (Table 4), the *qmax* for PAN-Na-Y adsorbent has 35.39, 40.69, and 35.07 mg/g as well as Mt-Chitosan has 49.33, 28.23, and 20.60 mg/g, respectively, for the removal of Pb(II), Cd (II) and Cu(II)[37,38]. The different Pb(II), Cd (II), and Cu(II) maximum adsorption capacities depended not only on the structure and morphology of the adsorbent, and the presence of functional groups but also on adsorption variables, such as pH, adsorbent dose, metal ions concentration, and contact time. The complexity was further caused by the non-uniformity of the maximum adsorption variable used and the various procedures the adsorption capacities were measured. Finally, in the choice selecting the appropriate adsorbent, availability, reusability, and cost-effectiveness were taken into account, which this adsorbent depicted. Therefore, it is noteworthy to mention that the adsorbent alg/Cs-NH_2-SiO_2/Fe_3O_4 has a promising potential for future use for Pb(II), Cd(II), and Cu(II), removal from effluent solution (Table 4).

Table 4. Comparative study of adsorption capacity of alg/Cs-NH_2-SiO_2/Fe_3O_4 adsorbent with similar adsorbents for the removal of Pb(II), Cd(II), and Cu(II) ions from aqueous solutions

Adsorbent	Metal Ions	q_{max} (mg/g)	pH	Isotherm/Kinetics	References
alg/Cs-NH_2SiO_2/Fe_3O_4	Pb (II)	41.79	6.0	Langmuir/	This study
	Cd (II)	39.21		Pseudo 2nd order	
	Cu (II)	39.56			
PAN-Na-Y	Pb (II)	35.39	6.0	Langmuir/	[37]
	Cd (II)	40.69		Pseudo 2nd order	
	Cu (II)	35.07			
Mt-Chitosan	Pb (II)	49.33	5.0	Langmuir/Freundlich	[38]
	Cd (II)	28.23		Pseudo 2nd order	
	Cu (II	20.60			
DTPA/MGO	Pb (II)	131.40	3.0	Langmuir/	(39)
	Cd (II)	387.60		Pseudo 2nd order	
	Cu (II	286.50			
Fe_3O_4-$FeMoS_4$	Pb (II)	190.75	5.0	Langmuir	[40]
	Cd (II)	140.50		Pseudo 2nd order	
	Cu (II	110.30			

Conclusion

In this paper, the novel effective adsorbent alg/Cs-NH_2-SiO_2/Fe_3O_4 adsorbent was successfully synthesized from Fe_3O_4, as a percussor coated with SiO_2, functionalized using APTES (-NH_2), and the blend combined with chitosan bound by alginate as a binder to form the biopolymer composite adsorbent. The adsorbent was characterized for the surface morphology, using FTIR, FESEM/EDX, and VSM methods which demonstrated a successful synthesis. The adsorbent was investigated with the batch method. The evaluation of alg/Cs-NH_2-SiO_2/Fe_3O_4 adsorption performance at optimized conditions of pH, time effect, adsorbent dosage, initial adsorbate concentration, and temperature. The findings revealed that the adsorbent has a maximum adsorption capacity of 41.79, 39.21, and 39.56 mg/g for Pb(II), Cu(II), and Cd(II), respectively. In addition, the adsorbent behavior was studied for the isotherm models using Langmuir, Freundlich, Temkin, and Dubinin-Rudushkevich's isotherm model**s**. Moreover, the results demonstrated that the isotherm and kinetic studies were better fitted to Langmuir isotherm and the pseudo-second order with the coefficient of determination (R^2) close to 0.999, indicating homogeneous surface and chemisorption. The adsorption-desorption experiment for five consecutive rounds of regeneration study was

conducted until a substantial change inthe performance of alg/Cs-NH_2-SiO_2/Fe_3O_4 was detected. Consequently, the findings revealed that the adsorbent still retained its adsorption ability achieved above 70%, after the 5th recycled, which indicated the efficiency of the adsorbent. In addition, the thermodynamic factors were investigated, and the results indicated endothermic and spontaneous processes. The industrial wastewater river area of Taman Mewah, Kulai, Johor, Malaysia for the application for the real sample, and the findings revealed that only Pb(II) was detected at 86% efficiency of removal. The adsorbent (alg/Cs-NH_2-SiO_2/Fe_3O_4) adsorption capacity towards Pb(II), Cd (II), and Cu(II) were compared with other adsorbents in literature and was ranked good among its contemporaries. Therefore, it is noteworthy to mention that the adsorbent alg/Cs-NH_2-SiO_2/Fe_3O_4 has a promising potential for future use for Pb(II), Cd(II), and Cu(II), removal from effluent solution.

Acknowledgment

We are grateful for the financial support of the work by Universiti Teknologi Malaysia via Universiti Teknologi Malaysia Fundamental Research grant (UTMFR, Q.J130000.2554.20H98, reference number PY/2019/02057) and UTMShine grant (Q.J130000.2454.09G30, reference number PY/2020/03555).

References

1. Rajapaksha, P. P., Power, A., Chandra, S. and Chapman, J. (2018). Graphene, electrospun membranes, and granular activated carbon for eliminating heavy metals, pesticides, and bacteria in water and wastewater treatment processes. *Analyst Journal*, 143(23): 5629-5645.
2. Sherlala, A. I. A., Raman, A. A. A., Bello, M. M. and Asghar, A. (2018). A review of the applications of organo-functionalized magnetic graphene oxide nanocomposites for heavy metal adsorption. *Chemosphere,* 193:1004–1017.
3. Kumar, R., Kumar, S., Guglani, S., Roy, S., Kaushik, B. K., Sharma, R., et al. (2020) Temperature-aware compact modeling for resistivity in ultra-scaled cu-graphene hybrid interconnects. SPI 2020 - 24th IEEE Work Signal Power Integrity, Proceeding (January 2021): pp. 1-8.
5. Mishra, S., Bharagava, R. N., More, N., Yadav, A., Zainith, S., Mani, S., et al. (2019) Heavy metal contamination: An alarming threat to environment and human health. *Journal of Environmental and Biotechnology Sustainable Future*, 2019: 103-125.
6. Samadi, N., Hasanzadeh, R. and Rasad, M. (2015). Adsorption isotherms, kinetic, and desorption studies on removal of toxic metal ions from aqueous solutions by the polymeric adsorbent. *Journal of Applied Polymer Science*, 132(11):1-13.
7. Sadati, B. N., Rostamizadeh, K., Yaftian, M. R., Zamani, A. and Ahmadi, H. (2014). Covalently modified magnetite nanoparticles with PEG: Preparation and characterization as nano-adsorbent for removal of lead from wastewater. *Journal of Environmetal Health Sciences Engineering,* 12(1): 103.
8. Ahmad, N., Sereshti, H., Mousazadeh, M., Rashidi, N. H., Kamboh, M. A. and Mohamad, S. (2018). New magnetic silica-based hybrid organic-inorganic nanocomposite for the removal of lead(II) and nickel(II) ions from aqueous solutions. *Journal of Material Chemistry and Physics*, 226:73-81.
9. Kariuki, Z., Kiptoo, J. and Onyancha, D. (2017). Biosorption studies of lead and copper using rogers mushroom biomass 'Lepiota hystrix.' *South African Journal of Chemcal Engineering*, 23:62-70.
10. Zulfiqar, A. S., Athar, M., Salman, M. and Imran, D. M. (2017) Simultaneous removal of Pb(II), Cd(II), and Cu(II) from aqueous solutions by adsorption on Triticum aestivum - a green approach. *Journal Hydrology Current Research*, 2(4): 4-11.
11. Prasath, R. R., Muthirulan, P. and Kannan, N. (2014). Agricultural wastes as a low cost adsorbent for the removal of Acid Blue 92 dye: A comparative study with commercial activated carbon. *IOSR Journal of Agriculture and Veternary Science,* 7(2):19-32.

12. Sutirman, Z. A., Sanagi, M. M., Abd Karim, K. J., Wan, I. W. A. and Jume, B. H. (2018) Equilibrium, kinetic and mechanism studies of Cu(II) and Cd(II) ions adsorption by modified chitosan beads. *International Journal Biological Macromolecules,* 116: 255-263.
13. Noor, N. M., Othman, R., Mubarak, N. M. and Abdullah, E. C. (2017). Agricultural biomass-derived magnetic adsorbents: Preparation and application for heavy metals removal. *Journal of the Taiwan Institute of Chemical Engineers*, 78: 168-177.
14. Ng, N. T., Kamaruddin, A. F., Wan, I. W. A., Sanagi, M. M. and Abdul Keyon, A. S. (2018) Advances in organic-inorganic hybrid sorbents for the extraction of organic and inorganic pollutants in different types of food and environmental samples. *Journal of Separation Science*, 41: 195-208.
15. Wang, J., Zheng, S., Shao, Y., Liu, J., Xu, Z. and Zhu, D. (2010). Amino-functionalized Fe_3O_4@SiO_2 core-shell magnetic nanomaterial as a novel adsorbent for aqueous heavy metals removal. *Journal of Colloid Interface Science*, 349(1):293-299.
16. Jahanbakhsh, Z., Hosseinzadeh, H., Masoumi, B. (2021). Synthesis of carboxymethyl β-cyclodextrin bonded Fe_3O_4@SiO_2–NH_2 core-shell magnetic nanocomposite adsorbent for effective removal of Pb(II) from wastewater. *Journal of Sol-Gel Science and Technology*, 99(1): 230-242.
17. Lim, J. W., Kim, T. Y. and Woo, M. A. (2021) Trends in sensor development toward next-generation point-of-care testing for mercury. *Journal of Biosensors and Bioelectronics,* 183:113228.
18. Ahmad, S. Z. N., Wan, S. W. N., Ismail, A. F., Yusof, N., Mohd, Y. M. Z. and Aziz, F. (2020). Adsorptive removal of heavy metal ions using graphene-based nanomaterials: Toxicity, roles of functional groups and mechanisms. *Chemosphere Journal*, 248: 126008.
19. Yang, L., Tian, J., Meng, J., Zhao, R., Li, C., Ma, J., et al. (2018). Modification and characterization of Fe_3O_4 nanoparticles for use in adsorption of alkaloids. *Journal of Molecules*, 23(2): 562.
20. Abbaszadeh, S., Nodeh, H. R. and Alwi, S. R. W. (2018). Bio-adsorbent derived from papaya peel waste and magnetic nanoparticles fabricated for lead determination. *Journal of Pure and Applied Chemistry*. 90(1):79-92.
21. Rahimdad, N., Khalaj, A., Azarian, G. and Nematollahi, D. (2019). Electrochemical device for the synthesis of Fe_3O_4 magnetic nanoparticles. *Journal of the Electrochemical Society*, 166(2): 1-6.
22. Markus, A., Gbadamosi, A. O., Yusuff, A. S., Agi, A. and Oseh, J. (2018). Magnetite-sporopollenin/graphene oxide as new pre-concentration adsorbent for removal of polar organophosphorus pesticides in vegetables. *Journal of Environmetal Science Pollution and Research*. 25(35): 35130-35142.
23. Alizadeh. A., Khodaei, M. M., Beygzadeh, M., Kordestani, D. and Feyzi, M. (2012). Biguanide-functionalized Fe_3O_7/SiO_2 magnetic nanoparticles: An efficient heterogeneous organosuperbase catalyst for various organic transformations in aqueous media. *Bulletin of the Korean Chemical Society*, 33(8):2546-2552.
24. Li, Y., Tsend, N., Li, T. K., Liu, H., Yang, R., Gai, X., et al. (2019). Microwave-assisted hydrothermal preparation of rice straw hydrochars for adsorption of organics and heavy metals. *Journal of Bioresource and Technology*, 273(8): 136-143.
25. Haseen, U., Ali, S. G., Umar K., Ali, A., Ahmad, H. and Khan, H. M. (2021). Dimercaptosuccinic acid functionalized polystyrene column for trace concentration determination of heavy metal ions: Experimental and theoretical calculation studies. *Water (Switzerland),*13(21).
26. Hassan, A. M., Wan, I. W. A., Bakar, M. B., Sanagi, M. M., Sutirman, Z. A., Nodeh, H. R., et al. (2020) New effective 3-aminopropyltrimethoxysilane functionalized magnetic sporopollenin-based silica coated graphene oxide adsorbent for removal of Pb(II) from aqueous environment. *Journal of Environmental Management,* 253(10): 109658.

27. Ahmad, N. F., Kamboh, M. A., Nodeh, H. R., Halim, S. N. B. A. and Mohamad, S. (2017). Synthesis of piperazine functionalized magnetic sporopollenin: a new organic-inorganic hybrid material for the removal of lead(II) and arsenic(III) from aqueous solution. *Journal of Environmental Science and Pollution Research,* 24(27): 21846-21858.
28. Nasirimoghaddam, S., Zeinali, S. and Sabbaghi, S. (2015). Chitosan coated magnetic nanoparticles as nano-adsorbent for efficient removal of mercury contents from industrial aqueous and oily samples. *Journal of Industrial and Engineering Chemistry*, 27: 79-87.
29. Upadhyay, U., Sreedhar, I., Singh, S. A., Patel, C. M. and Anitha, K. L. (2021). Recent advances in heavy metal removal by chitosan-based adsorbents. *Journal of Carbohydrate Polymer,* 251(8): 117000.
30. Kloster, G. A., Mosiewicki, M. A and Marcovich, N. E. (2019). Chitosan/iron oxide nanocomposite films: Effect of the composition and preparation methods on the adsorption of congo red. *Journal of Carbohydrate Polymer,* 221(3):186-194.
31. Wang, J., Zheng, C., Ding, S., Ma, H. and Ji, Y. (2011). Behaviors and mechanisms of tannic acid adsorption on an amino-functionalized magnetic nano adsorbent. *Journal of Desalination*, 273(2–3): 285-291.
32. Li, X., Wu, X., Chen, J., Li, Y. and Yang, Y. (2019) Alginate-enfolded copper hexacyanoferrate graphene oxide granules for adsorption of low-concentration cesium ions from the aquatic environment. *Journal of Radioanalytical and Nuclear Chemistry*, 320(3): 655-63.
33. Fýl, B. A., Boncukcuoglu, R., Yilmaz, A. E. and Bayar, S. (2012) Adsorption kinetics and isotherms for the removal of zinc ions from aqueous solutions by an ion-exchange resin. *Journal of Chemical Society of Pakistan*, 34(4): 841-848.
34. Nasir, A. M., Md, N. N. A. H., Goh, P. S. and Ismail, A. F. (2018) Application of two-dimensional leaf-shaped zeolitic imidazolate framework (2D ZIF-L) as arsenite adsorbent: Kinetic, isotherm, and mechanism. *Journal of Molecular Liquids,* 250: 269-277.
35. Gubbuk, I. H. (2011). Isotherms and thermodynamics for the sorption of heavy metal ions onto functionalized sporopollenin. *Journal of Hazardous Materials*, 186(1):416-22.
36. Sutirman, Z. A., Sanagi, M. M. and Wan, A.W. I. (2021). Alginate-based adsorbents for removal of metal ions and radionuclides from aqueous solutions: A review. *International Journal Biological Macromolecules,* 174: 216-228.
37. Elwakeel, K. Z., El-Bindary, A. A., Kouta, E. Y. and Guibal, E. (2018). Functionalization of polyacrylonitrile/Na-Y-zeolite composite with amidoxime groups for the sorption of Cu(II), Cd(II) and Pb(II) metal ions. *Chemical Engineering Journal*, 332(7): 727-236.
38. Hu, C., Zhu, P., Cai, M., Hu, H. and Fu, Q. (2017). Comparative adsorption of Pb(II), Cu(II), and Cd(II) on chitosan saturated montmorillonite: Kinetic, thermodynamic and equilibrium studies. *Applied Clay Science Journal,* 143(4): 320-326.
39. Li, X., Wang, S., Liu, Y., Jiang, L., Song, B., Li, M., et al. (2017). Adsorption of Cu(II), Pb(II), and Cd(II) ions from acidic aqueous solutions by diethylenetriaminepentaacetic acid-modified magnetic graphene oxide. *Journal of Chemical Engineering Data*, 62(1): 407-416.
40. Behbahani, E. S., Dashtian, K. and Ghaedi, M. (2021). Promise magnetite LDH-based adsorbent for simultaneous removal of Pb(II), Cd(II), and Cu(II) heavy metal ions. *Journal of Hazardous Materials*, 410(11): 124560.